On the role of capillary and viscous forces on wear and frictional performances of natural fiber composites under lubricated polishing

Faissal Chegdani[a,*], Mohamed El Mansori[a,b], Mahmoud Taki[c], Ramsey Hamade[c]

[a]Arts et Metiers Institute of Technology, MSMP, HESAM University, F-51006 Châlons-en-Champagne, France
[b]Texas A&M Engineering Experiment Station, College Station, TX 77843, USA
[c]American University of Beirut, Mechanical Engineering Department, Beirut – 1102, Lebanon

Abstract

This paper aims to investigate the frictional and wear performances of natural flax fibers reinforced polypropylene composites subjected to lubricated mechanical polishing. Particularly, the interactions between the biocomposite surfaces and two different liquids (oil and water) are considered using a rotary tribometer where the counter-face is fed by silicon carbide (SiC) abrasive papers. Friction and wear at dry, water and oil-lubricated polishing are hence studied. The biocomposite worn surfaces are examined using a scanning electron microscope (SEM) and an atomic force microscope (AFM). Results show a significant influence of the lubricant type on the wear and frictional performances of flax fiber composites. The lubricated friction behavior is dependent on both the hydrophilic and oleophilic properties of flax fibers. In addition to the abrasive wear, while the thermal softening of the biocomposite controls the adhesive wear mechanism at dry polishing, changing the lubricant type from water to oil leads to modify the adhesive wear sources from only capillary forces to capillary and viscous forces, which contributes to increasing the wear of flax fiber composites under oil-lubricated polishing.

Keywords

Polymer-matrix composite; Natural fibers; Lubricated wear; Mechanical polishing; Nanoindentation.

* Corresponding author: F. Chegdani (faissal.chegdani@ensam.eu)

1. Introduction

The potential use of natural fiber composites (biocomposites) in industrial applications is directly related to the success of secondary manufacturing of these ecofriendly materials. Biocomposites, especially those with long continuous natural fibers, present many challenges during near net shape processing where requirements include accurate dimensional tolerancing, drilling holes for assembly, and controlled surface characteristics [1–3]. Finishing operations such as machining or polishing are mandatory for fabricating the biocomposite part to meet service requirements [4,5].

However, finishing operations should not cause excessive damages to preserve the required industrial functionality of the biocomposite part (i.e. mechanical, frictional, thermal, acoustic, hygroscopic, or damping properties). The main damage source emanates from the severe contact between the abrasive tools and the biocomposite due to the high generated tribological and thermal stresses. In conventional materials, such issues are typically handled by using fluid (water- or oil-based) lubrication [6–9]. Utilizing lubricants in the processing of biocomposite materials is not straightforward given that the hydrophilic/oleophilic properties of natural fibers are not well mastered. The cellulosic structure of natural fibers is prone to water absorption (as moisture content) from the humid environment [10]. The absorbed water molecules can affect the physical and the mechanical properties of natural fibers and their composites at different scale levels by plasticizing the polymeric fiber components, modifying the cellulosic arrangement, and hydrolyzing the polymer matrix near the interfaces [11–15]. Few literature reports indicate that natural fibers can absorb oil [16,17]. This oleophilic property allows them to be used as natural adsorbent material for the removal of oil spills [18–20]. The literature does not report on how the oleophilic properties of natural fibers may influence their mechanical performance. Youssif and Nirmal [21] have investigated wear and frictional performance (with dry sliding) of oil palm fibers reinforced polyester composites after being aged in different types of solutions (i.e. water, salt water, diesel, petrol, and engine oil) for three years. It was found that the absorption of water exceeds that of oil fluids. This was due to the fact that cellulose, hemicellulose, and lignin have polar hydroxyl groups that are highly attractive to the hydrogen bonds of water [21–24]. These polar hydroxyl groups are less attracted to oil solutions and the low absorption rate of oil fluids is due to the oil molecules trapped on the composite surfaces [21]. Dry sliding tests in [21] show a high specific wear rate of oil palm fiber composite specimens aged in water solutions compared to those aged in oil solutions which can be due to the important damage that water can introduce to both natural fibers and the interfaces [22,25].

Furthermore, oil palm fiber composites aged in water solutions exhibit a higher friction coefficient than those in oil solutions which could be due to the higher viscosity of the oil molecules at the contact interface.

However, the tribological testing configuration of [21] is not transferable to a lubricated contact because sliding experiments were performed at dry conditions without any lubricant and the long time aging process (3 years) would not have the same impact on the biocomposite specimens as fluid lubrication during the finishing process. Moreover, the target objectives, as well as the physical mechanisms in the mechanical polishing process, are usually different than those in the tribological setting experiments. Indeed, the conventional tribological methods are employed for the investigation and the simulation of friction and wear processes of two surfaces in contact under sliding conditions [26]. In mechanical polishing processes, high material removal rates combined with good surface qualities are usually desirable as a result. The primary mechanism of material removal in mechanical polishing is the abrasion of the workpiece surface employing abrasive particles while sliding and rolling phenomena occur at the tool and workpiece interface due to relative motion between them against the applied load [27]. Unlike the conventional tribological setting where the heat generation is mostly caused by friction, the heat generation in mechanical polishing is produced by both friction and high plastic deformation rate. For all these reasons, understanding the wear and the frictional performances of biocomposites during finishing processes using the conventional tribological settings is not appropriate.

With the mechanical abrasive polishing process, this work investigates the effect of the lubrication fluid type on frictional and wear performances of biocomposite materials. Flax fibers reinforced polypropylene (PP) composites are considered in this study. Friction coefficient and specific wear rate values are obtained from an instrumented mechanical polishing setup. Scanning electron microscope (SEM) and the atomic force microscope (AFM) are used to characterize the wear signature of the biocomposite surfaces and for performing nanoindentation measurements, respectively. Using a 3D interferometer, the surface topography of the polished biocomposite surfaces is further quantified.

2. Materials and methods

Biocomposite specimens used in this study are elaborated with 40% *vt* of unidirectional flax fibers and 60% *vt* of polypropylene matrix using the thermocompression technique. The biocomposite sheets were supplied from “Composites Evolution” company in the United Kingdom. They are then cut into small samples with the dimensions 15×10×4 mm using an electrical saw. The unidirectional flax fibers are perpendicular to the worksurface as shown in Figure 1(a). Unlike synthetic fibers (glass or carbon), natural flax fibers are gathered in bundles of several elementary fibers as shown in Figure 1(b) that also reveals another particularity of natural fibers which is the random size and shape of the elementary fibers inside the same bundle.

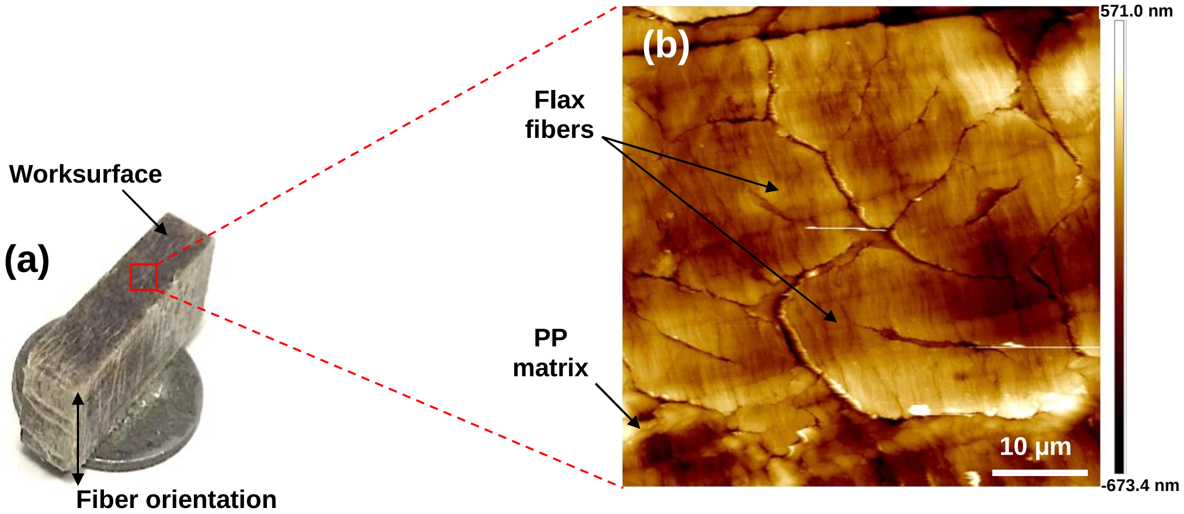

Figure 1: (a) photograph of the biocomposite specimens used in polishing experiments, (b) scanning probe image of the biocomposite surface showing cross-sections of flax fibers and PP matrix

Polishing experiments were conducted using a rotary pin-on-disc tribometer from “CSM Instruments” company (Ref. THT 03-111) where the counter-face is fed by silicon carbide (SiC) abrasive paper as shown in Figure 2. The surface forming from the raw cut surface (obtained with the electrical saw) to the final polished surface follows the steps described in Figure 3. Each specimen was subjected to a four-stage polishing procedure in which each stage contained a variety of conditions regarding the abrasive grit size, sliding distance, and polishing cycles. The procedure of Figure 3 was conducted under a constant load of 20N for three values of sliding speed (30 m/min, 35 m/min, and 40 m/min) and three lubrication conditions (dry, water lubrication, and oil lubrication). The selected approach uses a dynamic load effect in existence at the time of friction under dry and lubricated contact by keeping the normal load constant and changing the sliding speed. The oil used in this study is “Castrol

Honilo 981” which is applicable for fine machining and honing processes. It has a kinematic viscosity of 5 mm^2/s at 40°C.

After each cycle of each step in the polishing procedure, the corresponding abrasive paper is changed to avoid its saturation. The sliding distance of each step was defined at the saturation of the abrasive paper. Water and oil lubrication was carried out by introducing 3 ml of the stationary fluid in the container including the abrasive paper as shown in Figure 2(b).

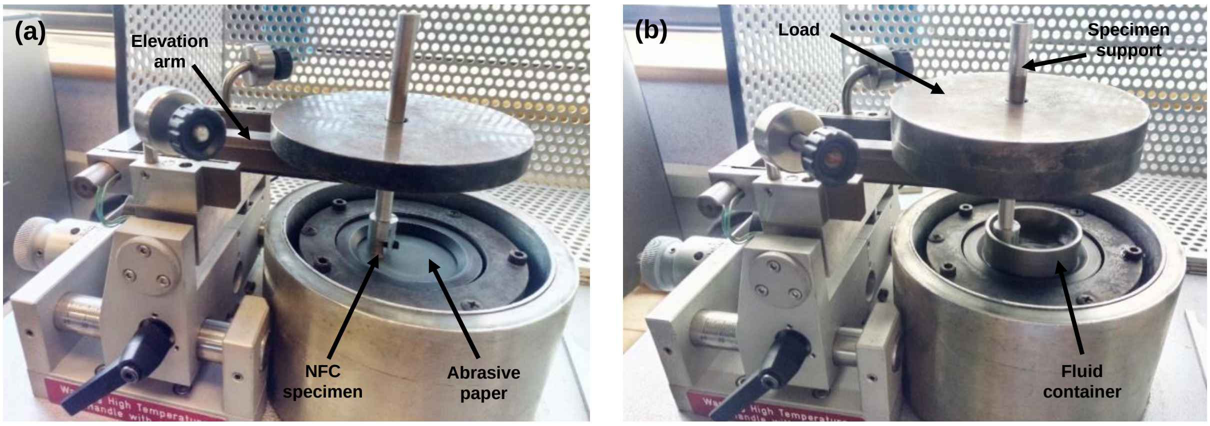

Figure 2: Experimental setup for (a) dry polishing and (b) water and oil lubricated polishing with a fluid container.

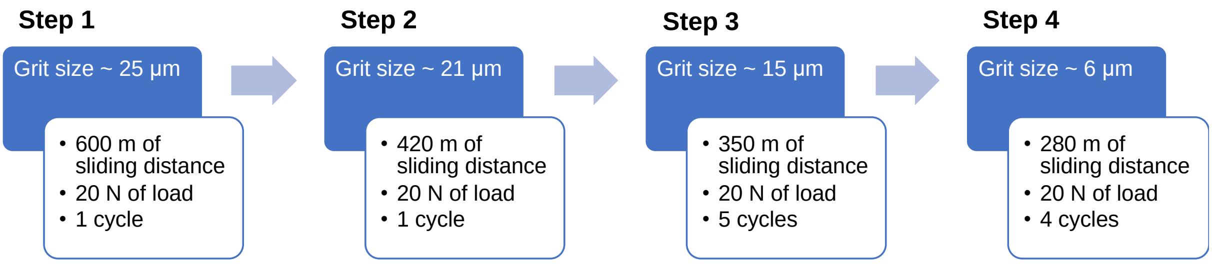

Figure 3: Schematic graph of the experimental procedure for the polishing tests

In situ friction coefficient was obtained by calculating the ratio of the tangential friction force (recorded with o rotary torque-meter) and the normal force for the contact between the biocomposite specimen and the abrasive counter-face. Specific wear rate (W_s) of biocomposite samples was calculated using the following equation (1) where ΔV is the removed volume, F_N is the applied load, and D is the sliding distance [21].

$$W_s = \frac{\Delta V}{F_N \, . \, D} \quad (1)$$

To get reliable results, each considered polishing configuration (from step1 to step 4) is repeated three times under identical conditions. Thus, the output values from polishing experiments are presented as the mean of these three repeated tests. Errors are considered as the average of the absolute deviations of data repeatability tests from their mean.

Microscopic observations of biocomposite polished surface state were made by a scanning electron microscope (SEM / JSM — 5510LV) at low vacuum mode. Typical representative surface morphology as induced by the polishing process of each experimental configuration was taken into account for the microscopic analysis.

Nanoindentation tests were conducted using an atomic force microscope (AFM) instrument (*Dimension Edge* from Bruker) with a Berkovich silicon tip indenter and a small tip radius (~ 20 nm). The tip indenter is related to a silicon cantilever that has a spring constant of 200 N/m. Nanoindentation experiments are carried out to measure the elastic modulus of the polished surfaces using the loading/unloading curves of each nanoindentation test [28,29]. More details on the elastic modulus calculation procedure from the nanoindentation curves can be found in [30].

Indentation tests are performed on flax fibers and PP matrix separately for the resulting surface of each polishing configuration. Three to four regions on each biocomposite surface are scanned using AFM Tapping mode with an image size of 30 μm^2. Depending on the fiber size in the scanned region, from 15 to 50 indentations are executed on each cross-section of flax fibers. For the PP matrix, about 50 indentations are made on each scanned region of the polymer.

Friction and wear analysis are performed on step 4 of the polishing procedure (the smallest grit size) while SEM, AFM, and topographic measurements are made on the final surfaces of each polishing configuration.

3. Results and discussion

3.1. Polishing-induced damages on biocomposite surfaces

Figure 4 presents the microscopic aspect of the polished surfaces at the different lubrication and sliding speed conditions. The cross-sections of flax fibers obtained by water-lubricated polishing are the cleanest (Figure 4(c,d)), while the worst cross-sections of flax fibers are those achieved by dry polishing because they suffer from plastic deformation at the polished surface as shown in Figure 4(a,b). This is due to the thermal effect induced by the abrasion of fibers under dry friction. Indeed, dry polishing generates high temperature at the contact interface between the biocomposite and the counter-face which softens the natural polymeric composition of flax fibers (hemicellulose, lignin, and pectin) and favors its plastic deformation. The presence of water as a lubricant avoids the high increase of temperature at the contact interface which prevents the plastic deformation phenomenon. Water-lubricated polishing induces fractures in the polymer (PF in Figure 4(c,d)) and the interfaces (IF in Figure 4(c,d). This damage phenomenon could be explained by the surface hardening. Performing the polishing process with water lubrication will deform the biocomposite surface without a high-temperature increase (i.e. without material softening) which leads to harden the composite surface and make it more brittle against the severe undergoing mechanical stresses. This has a clear impact on the polymer matrix and the interfaces as shown in Figure 4(c,d).

Abrasive debris (from the abrasive papers of the counter-face) are highly present on the surfaces polished by oil lubrication (Figure 4(e,f)). Dry polishing shows also the presence of debris but lower than that of oil-lubricated polishing, while water-lubricated polishing exhibits the lowest rate of debris that is visible only at the highest sliding speed of 40 m/min. This indicates that the use of water as lubricant avoids the trapping of the abrasive debris on the biocomposite surfaces after polishing.

It can also be noted that increasing the sliding speed increases the damages for all the lubrication conditions such as abrasive debris, polymer fracture, interfaces fracture, in addition to some hollow spots that appear on the surfaces polished using oil lubrication (HS in Figure 4(f)) which may be due to the torn-off of flax fibers.

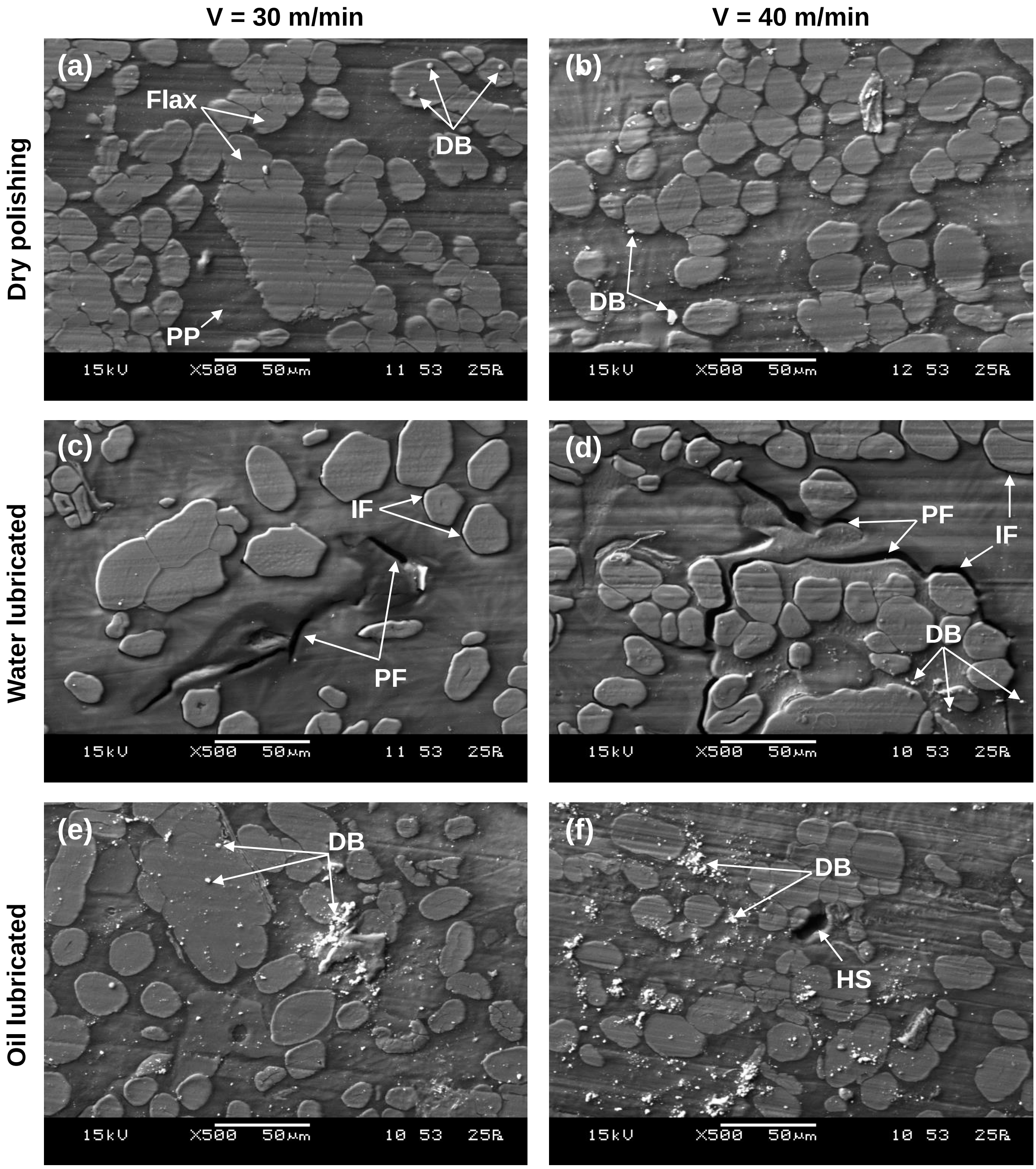

Figure 4: Typical SEM images of the polished surfaces with different lubrication and sliding speed conditions. DB: debris, PF: polymer fracture, IF: interfaces fracture, and HS: hollow spot

3.2. Lubrication effect on friction performances

The coefficient of friction (COF) signals at step 4 of the polishing procedure are illustrated in Figure 5. The COF signals show a steady-state regime after about 50 m of sliding distance. The COF signals of dry polishing present high fluctuations, especially at the first repetition. The COF signal fluctuations decrease with increasing the polishing cycles. The smallest COF signal fluctuations are observed for oil-lubricated polishing where the four friction cycles seem to be quasi similar. The highest instability observed in the dry polishing signals of the COF could be due to the initial surface irregularities obtained from step 3 of the polishing procedure. Introducing fluid lubrication reduced this contact variability by filling in the streaks induced in step 3 of the polishing procedure. The fluctuation in the COF signals is more reduced by oil lubrication thanks to its viscosity. Figure 5 implies that dry polishing induces, in general, the highest COF values while oil-lubricated polishing induces the lowest COF values.

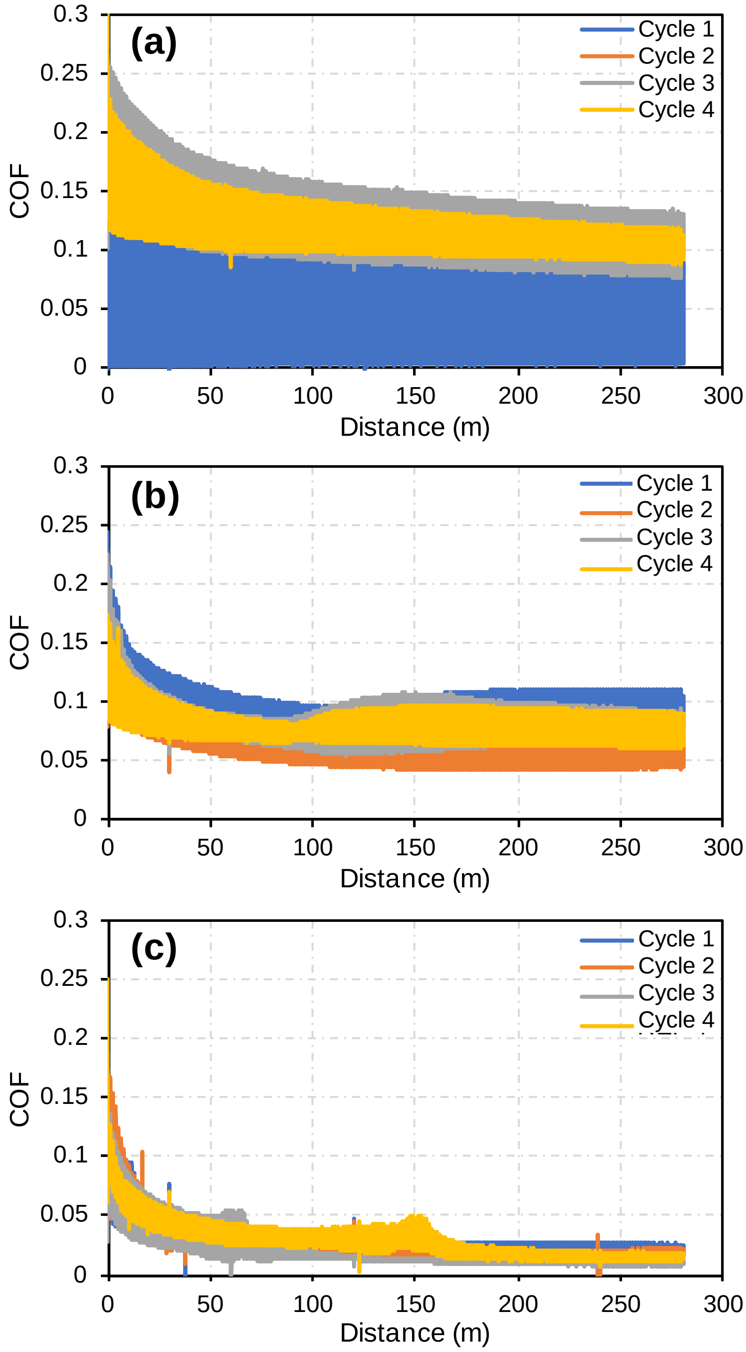

Figure 5: Friction coefficient signal of step 4 of the polishing procedure for (a) dry polishing, (b) water-lubricated polishing, and (c) oil-lubricated polishing

For each of the three polishing configurations, Figure 6 presents the average of the mean COF values of the four polishing cycles shown in Figure 6 at the steady-state regime. The frictional behavior in dry polishing is most influenced by the sliding speed where the COF increases by increasing the sliding speed. The COF due to oil-lubricated polishing slightly increases with sliding speed increase. The COF due to water-lubricated polishing appears to be independent of sliding speeds between 30 m/min and 40 m/min.

The frictional behavior of flax/PP composites against lubrication is in good agreement with that of conventional materials such as metals [31], polymers [32], and synthetic fiber composites [33,34]. Dry polishing induces high temperature at the contact interface which softens the polymeric compositions of the biocomposite in this contact zone as for the common polymeric materials [35,36]. Therefore, the surface of the biocomposite will become more ductile and will easily adapt to the morphology of the abrasive counter-face. The contact area will consequently increase which will raise the friction force and generate the highest COF. Moreover, increasing the sliding speed will further raise the temperature in the contact zone, which contributes to the increase of the contact area, inciting an increase of the COF versus the sliding speed.

For liquid-lubricated polishing, the thin liquid film at the contact interface leads to a decrease in both the high shear stresses and the high induced temperatures during polishing which reduces the friction force. Due to its low viscosity, the lubrication film thickness of water is about 70 nm which is 1/100 to 1/1000 of the thickness of conventional oil in hydrodynamic lubrication conditions [37]. Moreover, the cellulosic structure of natural fibers gives them the ability to trap oil molecules on the worksurface [21] which further increases the oil film thickness formed at the polishing contact interface. This can explain the low values of COF in oil lubrication comparing to water lubrication.

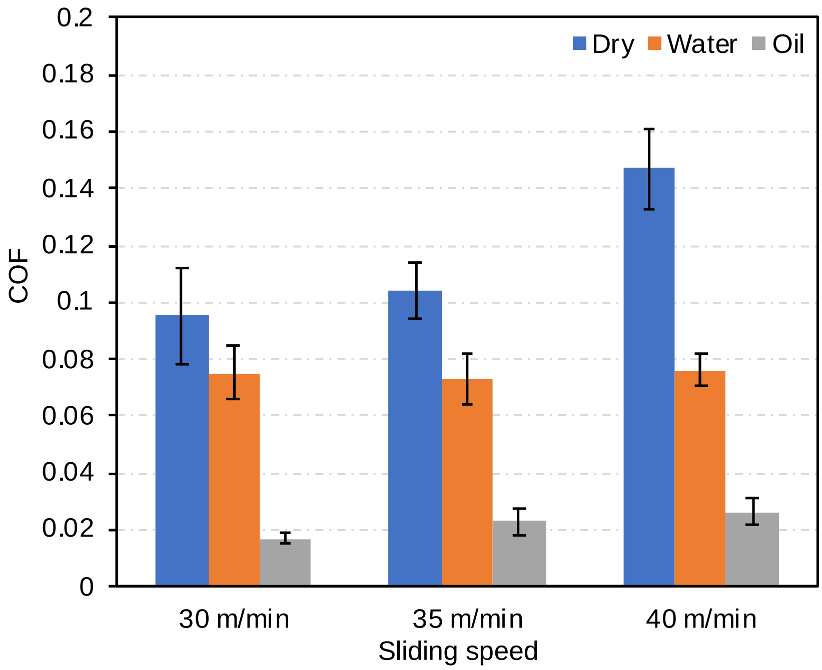

Figure 6: COF at the steady-state regime of step 4 of the polishing procedure of the biocomposites

3.3. Lubrication effect on wear performances

As for the COF analysis, the specific wear rate is calculated from the average of the removed volume in the four polishing cycles performed in step 4 of the polishing procedure. Figure 7 shows that dry polishing induces the lowest specific wear rate that is not significantly impacted by the increase of the sliding speed. Oil-lubricated polishing generates the highest specific wear rate that decreases by increasing the sliding speed. For water-lubricated polishing, the specific wear rate is similar to that of dry polishing at 30 m/min of sliding speed but increases by increasing the sliding speed to be notably higher than that of dry polishing at 40 m/min of sliding speed.

From the microscopic observations of Figure 4, the main wear mechanisms that occurred in the polishing process of flax/PP composites are adhesive wear, two-body abrasive wear, and three-body abrasive wear. Abrasive wear mechanisms are induced by the action of the SiC abrasive paper (two-body) and its debris (three-body) on the biocomposite surface, while adhesive wear is related to the contact nature that is controlled by the lubrication conditions. Adhesive wear is proportional to the adhesive force between the two surfaces in contact [38]. For liquid-lubricated polishing, the adhesive forces (F) that can be divided into two components: a capillary meniscus force (F_m) due to surface tension and a viscous force (F_v) related to the viscous movement of contacting liquid [39,40]. The viscous force is rate-dependent and is only significant for high-viscous liquid. The presence of the capillary condensation and liquid film could significantly increase the adhesion force between surfaces [41].

In the case of biocomposite materials, the capillary force can have an important role in the contact adhesion because of the hydrophilic properties of natural fibers. Indeed, natural plant fibers can be modeled at microscale as a capillary tube (cylinder with a central cavity called lumen [42,43]). The hydrophilic characteristics of the natural fiber components lead to water absorption inside the fiber structure and the hydroxyl groups present on the fiber surfaces increase the wettability of the fiber with water [44–46]. Therefore, when a capillary tube (i.e. elementary flax fiber) is dipped into a liquid and the liquid wets the tube (due to the hydrophilic properties of flax fibers), the liquid rises in the tube and the liquid surface inside the tube forms a concave meniscus, which is a virtually spherical surface having the same radius, r, as the inside of the tube [47,48]. The tube experiences a downward capillary force (F_m) expressed in equation (2), where σ is the surface tension of the liquid and θ is the contact angle [49].

$$F_m = 2\pi r\sigma \cos\theta \qquad (2)$$

The surface tension leads to increase adhesion for surfaces exposed to a high level of relative humidity promoting multilayer adsorption of water [39]. Since flax fibers are attractive for water with smaller wetting contact angle [46], F_m is the predominant adhesive force in water-lubricated polishing that contributes to increase the adhesive wear of flax fiber composites comparing to dry polishing. When using oil liquid as a lubricant, the viscous force (F_v) is activated and contributes to the adhesive force. F_v is defined by the equation (3) where β is a proportional constant, η_l is the dynamic viscosity of the liquid, and t_s is the time needed to separate the two surfaces [41]. The higher viscosity of oil lubricant, comparing to that of water, induces higher viscous force which increases the adhesive force and thus the adhesive wear generated by oil-lubricated polishing.

$$F_v = \frac{\beta\, \eta_l}{t_s} \qquad (3)$$

On the other hand, the abrasive debris highly present in oil-lubricated polished surfaces (Figure 4(e,f)) contribute to increasing the specific wear rate by acting as third abrasive bodies that accelerate the material removal rate from the biocomposite surfaces. Indeed, the abrasive wear process in polymers is traditionally divided into two groups: two-body and three-body abrasive wear. Two-body abrasion occurs when the wear is caused by hard particles fixed to the counter-face. This mechanism very often changes to three-body abrasion, where the wear particles act as abrasives between the two surfaces [50]. Water lubrication avoids a high rate of trapped abrasive particles on the biocomposite surface which reduces considerably this abrasive wear mechanism.

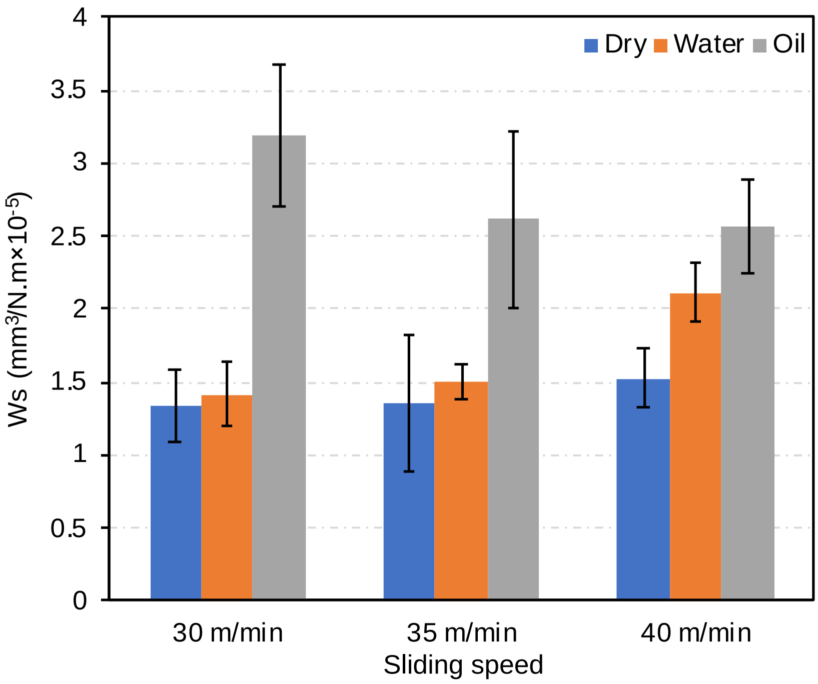

Figure 7: Specific wear rate at step 4 of the polishing procedure of the biocomposites

3.4. Lubrication effect on the mechanical damages

Figure 8 and Figure 9 present scanning images performed with the tapping mode of the AFM device. The AFM images show the indentation traces in addition to more microscopic details on the surface morphology and wear mechanisms of both flax fibers and PP matrix.

Figure 8 shows that dry and oil-lubricated polishing induced particular surface wear which is more intense in oil-lubricated surfaces, especially at the highest sliding speed. This wear phenomenon is due to the abrasive debris as discussed in section 3.3.

Elastic modulus results of the polished surfaces are presented in Figure 10 for flax fibers and PP matrix separately. Flax fibers processed with dry polishing exhibit the highest elastic modulus, followed by water-lubricated polishing and then oil-lubricated polishing (Figure 10(a)). For all the lubricated conditions on flax fibers, increasing the sliding speed decreases the elastic modulus. This indicates that the lubrication and sliding speed conditions have an impact on the induced mechanical damages of the flax fibers which is probably related to their absorption properties. Indeed, as explained in section 1, flax fibers can absorb water and oil from the external environment [16,17]. This liquid absorption leads to reduce the elastic properties of flax fibers by provoking their plasticization [51]. Increasing the sliding speed may accelerate the absorption kinetics in flax fibers, which increases their mechanical damages when using water or oil lubrication.

For oil-lubricated polishing, the high third-body abrasion rate observed in Figure 4(e,f) will further contribute to increasing the mechanical surface damage as shown in Figure 8(e,f), which can explain the lowest elastic modulus values of flax fiber for the oil-lubricated configurations.

In the PP matrix, the mechanical behavior is different because petrol-sourced polymers such as PP do not absorb liquid at their solid-state. At 30 m/min of sliding speed, the elastic modulus is similar for the three lubrication conditions as shown in Figure 10(b). A slight decrease of the elastic modulus in the function of the sliding speed is observed for dry and oil-lubricated polishing. For dry polishing, this is due to the thermomechanical damages induced by friction heat that increases by increasing the sliding speed. For oil-lubricated polishing, this mechanical behavior is probably due to the third-body abrasion damages that intensify when increasing the sliding speed as shown in the SEM images of Figure 4(e,f).

However, the elastic modulus of the PP matrix increases notably with sliding speed increase in the case of water-lubricated polishing. This behavior may be due to the surface hardening by plastic deformation in the absence of friction-induced heat, which is in good agreement with the brittle polymer fracture phenomenon observed in the SEM images of Figure 4(c,d) and discussed in section 3.1.

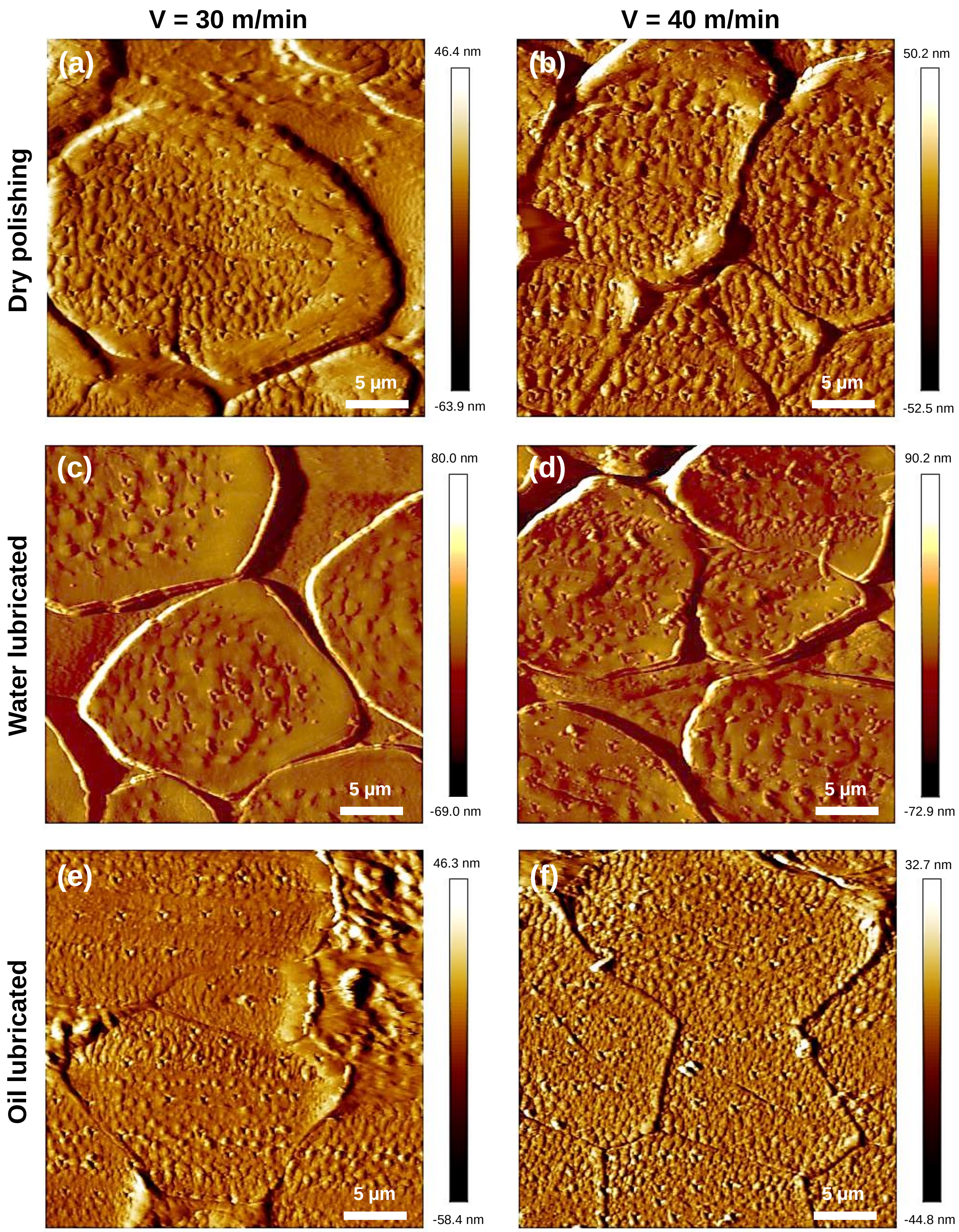

Figure 8: Scanning probe images with AFM of flax fiber cross-sections in polished surfaces obtained for different lubrication and sliding speed conditions

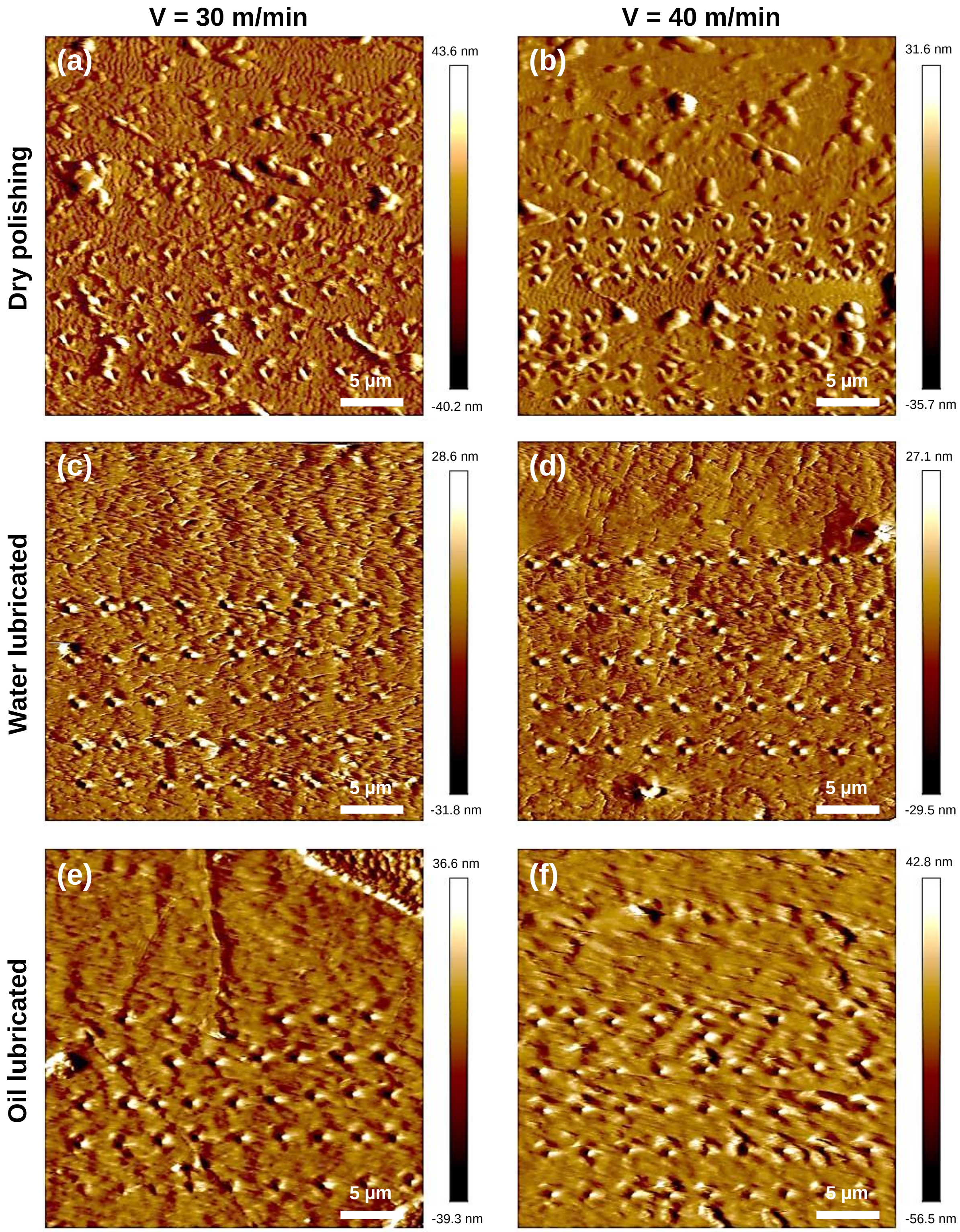

Figure 9: Scanning probe images with AFM of PP matrix in polished surfaces obtained for different lubrication and sliding speed conditions

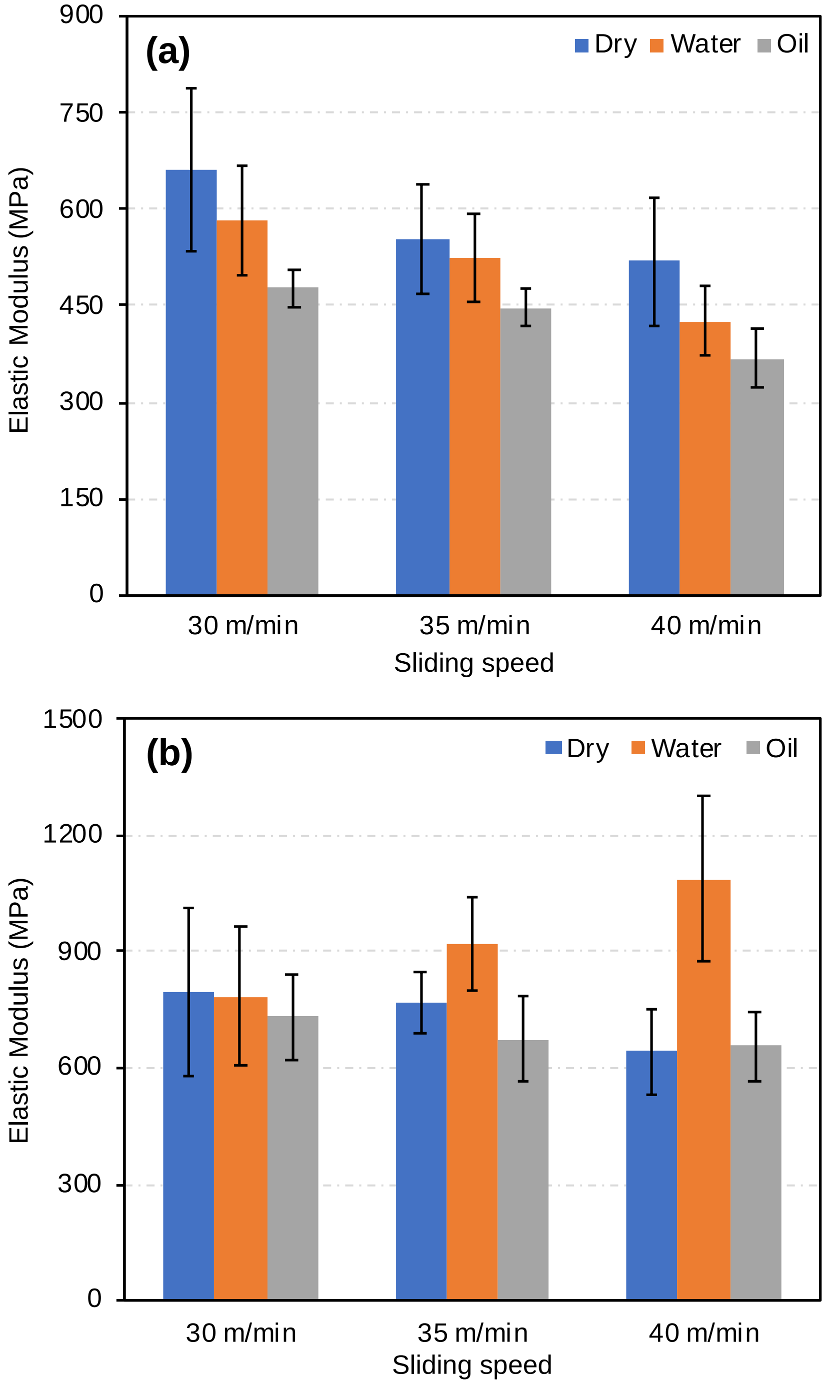

Figure 10: Elastic modulus obtained by AFM nanoindentation for (a) flax fibers, and (b) PP matrix

3.5. Lubrication effect on the polished surface roughness

To qualify the lubrication effect on the polished surface roughness of flax/PP composites, the topographic image size should correspond to the natural fibrous structure size to be on the relevant scale for an efficient topographic analysis of natural fiber composites [52]. The fibrous structure size in the case of the considered flax/PP composites are continuous unidirectional flax yarns that have an average diameter of about 1mm. The objective of the interferometer has been adapted to be as close as possible to this scale range. Therefore, an objective with a magnification of ×5 is used to get topographic images of 1 mm^2. The quantification of these 3D measurements with the arithmetic mean of the surface roughness (Sa) is given in Figure 11.

The surface roughness behavior of Figure 11 is in good agreement with the microscopic observations of Figure 4. Oil-lubricated polishing induces the highest surface roughness because of the high rate of trapped abrasive debris that increases when increasing the sliding speed. Water-lubricated polishing generates higher surface roughness than dry polishing because of polymer and interface fractures that are also intensified when increasing the sliding speed (see Figure 4). The low rate of trapped abrasive debris on the surfaces performed by dry polishing leads to engender the lowest roughness values.

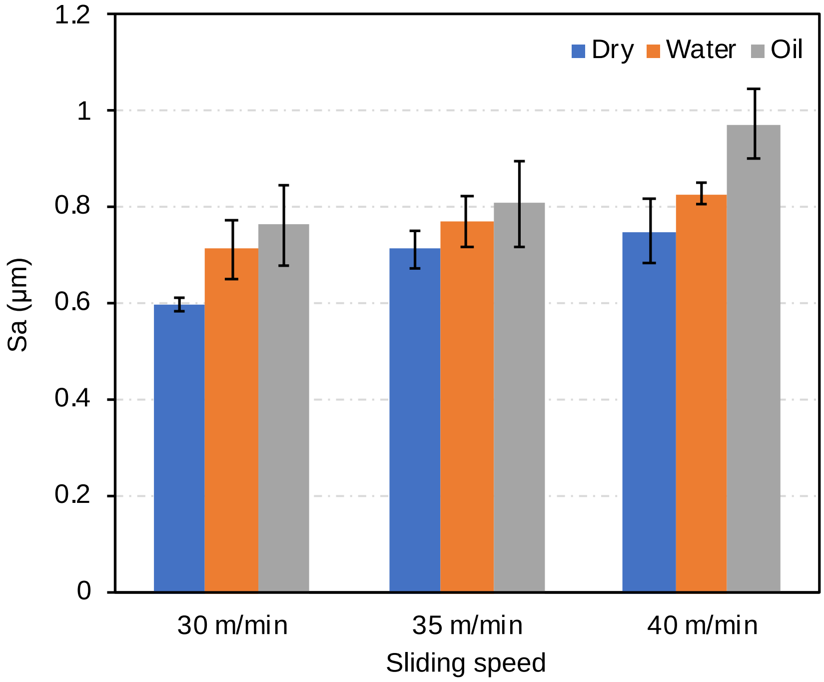

Figure 11: 3D arithmetic mean of the surface roughness for the resulting polished surfaces of the biocomposite

4. Conclusions

In this paper, the effect of lubrication conditions on frictional and wear performances of flax fiber reinforced polypropylene (PP) composites is investigated using the mechanical polishing process. The coefficient of friction (COF) and the specific wear rate are calculated from the instrumented experimental setup, while the polished surfaces are characterized using a scanning electron microscope (SEM) and atomic force microscope (AFM). Finally, the topographic surfaces as induced by the polishing process are accessed using a 3D interferometer. The following conclusions can be drawn:

- Frictional performances of flax fiber composites exhibit an important effect of the lubricant nature. Dry polishing induces the highest friction coefficient while oil-lubricated polishing shows the lowest friction coefficient despite it generates an important rate of abrasive debris. The ability of flax fibers to trap the oil molecules allows the formation of a thicker oil film that contributes to reducing the induced contact shear stresses.
- Wear performances of flax fiber composites regarding the lubrication conditions are related to the adhesive contact force that involves the contribution of the meniscus force (induced by the capillary effect of the fluid lubricant) and the viscous force (highly dependent on the viscosity of the fluid lubricant). Therefore, water lubrication shows the contribution of only the capillary meniscus force, while oil lubrication exhibits the association of the two components of the adhesive contact force.
- Dry and oil-lubricated polishing show the presence of trapped abrasive debris that act as a third abrasive body on the surface and then contribute to induce additional abrasive wear on the biocomposite surfaces. Water lubrication can avoid this abrasive wear issue but leads to generate fractures in both the polymer and the interfaces due to surface hardening.
- The hydrophilic/oleophilic properties of flax fibers contribute to increasing the mechanical damages on the polished surfaces of flax/PP composites when using fluid lubrication. Indeed, water and oil absorption of flax fibers from the lubricant decreases the elastic modulus of the polished surfaces. Oil-lubricated surfaces suffer also from mechanical degradation induced by the trapped abrasive debris.

5. References

[1] T. Rajmohan, R. Vinayagamoorthy, K. Mohan, Review on effect machining parameters on performance of natural fibre–reinforced composites (NFRCs), J. Thermoplast. Compos. Mater. 32 (2019) 1282–1302. https://doi.org/10.1177/0892705718796541.

[2] M.M.A. Nassar, R. Arunachalam, K.I. Alzebdeh, Machinability of natural fiber reinforced composites: a review, Int. J. Adv. Manuf. Technol. 88 (2017) 2985–3004. https://doi.org/10.1007/s00170-016-9010-9.

[3] R. Vinayagamoorthy, T. Rajmohan, Machining and its challenges on bio-fibre reinforced plastics: A critical review, J. Reinf. Plast. Compos. 37 (2018) 1037–1050. https://doi.org/10.1177/0731684418778356.

[4] F. Chegdani, S. Mezghani, M. El Mansori, A. Mkaddem, Fiber type effect on tribological behavior when cutting natural fiber reinforced plastics, Wear. 332–333 (2015) 772–779. https://doi.org/10.1016/j.wear.2014.12.039.

[5] F. Chegdani, M. El Mansori, Tribo-functional effects of double-crossed helix on surface finish, cutting friction and tool wear mechanisms during the milling process of natural fiber composites, Wear. 426–427 (2019) 1507–1514. https://doi.org/10.1016/j.wear.2018.11.026.

[6] Y.H. Wu, H.J. Yang, R.P. Guo, X.J. Wang, X.H. Shi, P.K. Liaw, J.W. Qiao, Tribological behavior of boronized Al0.1CoCrFeNi high-entropy alloys under dry and lubricated conditions, Wear. 460–461 (2020) 203452. https://doi.org/https://doi.org/10.1016/j.wear.2020.203452.

[7] M. Lou, D.R. White, A. Banerji, A.T. Alpas, Dry and lubricated friction behaviour of thermal spray low carbon steel coatings: Effect of oxidational wear, Wear. 432–433 (2019) 102921. https://doi.org/https://doi.org/10.1016/j.wear.2019.05.036.

[8] F. Itoigawa, T.H.C. Childs, T. Nakamura, W. Belluco, Effects and mechanisms in minimal quantity lubrication machining of an aluminum alloy, Wear. 260 (2006) 339–344. https://doi.org/https://doi.org/10.1016/j.wear.2005.03.035.

[9] K. Serpin, S. Mezghani, M. El Mansori, Multiscale assessment of structured coated abrasive grits in belt finishing process, Wear. 332–333 (2015) 780–787. https://doi.org/10.1016/j.wear.2015.01.054.

[10] W. WANG, M. SAIN, P. COOPER, Study of moisture absorption in natural fiber plastic composites, Compos. Sci. Technol. 66 (2006) 379–386. https://doi.org/10.1016/j.compscitech.2005.07.027.

[11] Y. Li, B. Xue, Hydrothermal ageing mechanisms of unidirectional flax fabric reinforced epoxy composites, Polym. Degrad. Stab. 126 (2016) 144–158. https://doi.org/10.1016/j.polymdegradstab.2016.02.004.

[12] M. Assarar, D. Scida, A. El Mahi, C. Poilâne, R. Ayad, Influence of water ageing on mechanical properties and damage events of two reinforced composite materials: Flax-fibres and glass-fibres, Mater. Des. 32 (2011) 788–795. https://doi.org/10.1016/j.matdes.2010.07.024.

[13] A. Regazzi, S. Corn, P. Ienny, J.-C.C. Bénézet, A. Bergeret, Reversible and irreversible changes in physical and mechanical properties of biocomposites during hydrothermal aging, Ind. Crops Prod. 84 (2016) 358–365. https://doi.org/10.1016/j.indcrop.2016.01.052.

[14] V. Placet, O. Cisse, M.L. Boubakar, Influence of environmental relative humidity on the tensile and rotational behaviour of hemp fibres, J. Mater. Sci. 47 (2012) 3435–3446. https://doi.org/10.1007/s10853-011-6191-3.

[15] A. Stamboulis, C.A. Baillie, T. Peijs, Effects of environmental conditions on mechanical and physical properties of flax fibers, Compos. Part A Appl. Sci. Manuf. 32 (2001) 1105–1115. https://doi.org/10.1016/S1359-835X(01)00032-X.

[16] N.A. Ahad, F.Z. Rozali, N.H. Rosli, N.I.H. Hanif, N. Parimin, Oil and water absorption behavior of tpu/natural fibers composites, Solid State Phenom. 280 SSP (2018) 374–381. https://doi.org/10.4028/www.scientific.net/SSP.280.374.

[17] N.A. Ahad, Oils and water absorption behavior of natural fibers filled TPU composites for biomedical applications In Press , Accepted Manuscript – Note to users Oils and water absorption behavior of natural fibers filled TPU composites for biomedical applications, in: J. Eng. Res. Educ., 2018: pp. 16–21.

[18] V. Fiore, E. Piperopoulos, L. Calabrese, Assessment of Arundo donax fibers for oil spill

recovery applications, Fibers. 7 (2019) 75. https://doi.org/10.3390/fib7090075.

[19] C. Wong, T. McGowan, S.G. Bajwa, D.S. Bajwa, Impact of fiber treatment on the oil absorption characteristics of plant fibers, BioResources. 11 (2016) 6452–6463. https://doi.org/10.15376/biores.11.3.6452-6463.

[20] O. Abdelwahab, S.M. Nasr, W.M. Thabet, Palm fibers and modified palm fibers adsorbents for different oils, Alexandria Eng. J. 56 (2017) 749–755. https://doi.org/10.1016/j.aej.2016.11.020.

[21] B.F. Yousif, U. Nirmal, Wear and frictional performance of polymeric composites aged in various solutions, Wear. 272 (2011) 97–104. https://doi.org/10.1016/j.wear.2011.07.006.

[22] A. Chilali, W. Zouari, M. Assarar, H. Kebir, R. Ayad, Effect of water ageing on the load-unload cyclic behaviour of flax fibre-reinforced thermoplastic and thermosetting composites, Compos. Struct. 183 (2018) 309–319. https://doi.org/10.1016/j.compstruct.2017.03.077.

[23] A. Le Duigou, P. Davies, C. Baley, Seawater ageing of flax/poly(lactic acid) biocomposites, Polym. Degrad. Stab. 94 (2009) 1151–1162. https://doi.org/10.1016/J.POLYMDEGRADSTAB.2009.03.025.

[24] H.N.N. Dhakal, Z.Y.Y. Zhang, M.O.W.O.W. Richardson, Effect of water absorption on the mechanical properties of hemp fibre reinforced unsaturated polyester composites, Compos. Sci. Technol. 67 (2007) 1674–1683. https://doi.org/10.1016/J.COMPSCITECH.2006.06.019.

[25] R.-H. Hu, M. Sun, J.-K. Lim, Moisture absorption, tensile strength and microstructure evolution of short jute fiber/polylactide composite in hygrothermal environment, Mater. Des. 31 (2010) 3167–3173. https://doi.org/10.1016/J.MATDES.2010.02.030.

[26] H. Kaleli, New universal Tribometer as pin or ball-on-disc and reciprocating pin-on-plate types, Tribol. Ind. 38 (2016) 235–240.

[27] B. Nayak, N. Ramesh Babu, Influence of tool and workpiece interface temperature rise on the life of ice bonded abrasive polishing tool, Wear. 462–463 (2020) 203511. https://doi.org/10.1016/j.wear.2020.203511.

[28] A. Bourmaud, S. Pimbert, Investigations on mechanical properties of poly(propylene) and poly(lactic acid) reinforced by miscanthus fibers, Compos. Part A Appl. Sci. Manuf. 39 (2008) 1444–1454. https://doi.org/10.1016/j.compositesa.2008.05.023.

[29] A.C. Fischer-Cripps, Nanoindentation Testing, in: Nanoindentation, Springer, New York, NY, 2011: pp. 21–37. https://doi.org/10.1007/978-1-4419-9872-9_2.

[30] A.Y. Jee, M. Lee, Comparative analysis on the nanoindentation of polymers using atomic force microscopy, Polym. Test. 29 (2010) 95–99. https://doi.org/10.1016/j.polymertesting.2009.09.009.

[31] P.J. Blau, Friction and wear of a Zr-based amorphous metal alloy under dry and lubricated conditions, Wear. 250–251 (2001) 431–434. https://doi.org/10.1016/S0043-1648(01)00627-5.

[32] J.K. Lancaster, A review of the influence of environmental humidity and water on friction, lubrication and wear, Tribol. Int. 23 (1990) 371–389. https://doi.org/10.1016/0301-679X(90)90053-R.

[33] B.F. Yousif, N.S.M. El-Tayeb, Effect of water as lubricant on friction and wear properties of CGRP composite evaluated by POD and BOR techniques, Surf. Rev. Lett. 14 (2007) 185–191. https://doi.org/10.1142/S0218625X07009244.

[34] S. Agrawal, K.K. Singh, P.K. Sarkar, Comparative investigation on the wear and friction behaviors of carbon fiber reinforced polymer composites under dry sliding, oil lubrication and inert gas environment, Mater. Today Proc. 5 (2018) 1250–1256. https://doi.org/10.1016/j.matpr.2017.11.208.

[35] C. Allen, A. Bloyce, T. Bell, Sliding wear behaviour of ion implanted ultra high molecular weight polyethylene against a surface modified titanium alloy Ti-6Al-4V, Tribol. Int. 29 (1996) 527–534. https://doi.org/10.1016/0301-679X(95)00116-L.

[36] J. Huang, X. Zhou, J. Wang, X. Tang, F. Kuang, Influence of temperature on friction of polymeric materials in water, Wear. 426–427 (2019) 868–876. https://doi.org/10.1016/j.wear.2019.01.115.

[37] H.J. Kim, D.E. Kim, Water lubrication of stainless steel using reduced graphene oxide coating, Sci. Rep. 5 (2015). https://doi.org/10.1038/srep17034.

[38] H. Mishina, A. Hase, Effect of the adhesion force on the equation of adhesive wear and the generation process of wear elements in adhesive wear of metals, Wear. 432–433 (2019)

202936. https://doi.org/10.1016/j.wear.2019.202936.

[39] S. Mirzababaei, P. Filip, Impact of humidity on wear of automotive friction materials, Wear. 376–377 (2017) 717–726. https://doi.org/10.1016/j.wear.2017.02.020.

[40] S. Cai, B. Bhushan, Meniscus and viscous forces during separation of hydrophilic and hydrophobic smooth/rough surfaces with symmetric and asymmetric contact angles, Philos. Trans. R. Soc. A Math. Phys. Eng. Sci. 366 (2008) 1627–1647. https://doi.org/10.1098/rsta.2007.2176.

[41] G. Sheng Chen, X. Liu, G. Sheng Chen, X. Liu, Chapter 3 – Friction, in: G. Sheng Chen, X.B.T.-F.D. Liu (Eds.), Frict. Dyn., Woodhead Publishing, 2016: pp. 91–159. https://doi.org/10.1016/B978-0-08-100285-8.00003-1.

[42] C. Baley, Analysis of the flax fibres tensile behaviour and analysis of the tensile stiffness increase, Compos. - Part A Appl. Sci. Manuf. 33 (2002) 939–948. https://doi.org/10.1016/S1359-835X(02)00040-4.

[43] M. Zimniewska, M. Wladyka-Przybylak, J. Mankowski, Cellulosic Bast Fibers, Their Structure and Properties Suitable for Composite Applications, in: Cellul. Fibers Bio- Nano-Polymer Compos., Springer Berlin Heidelberg, Berlin, Heidelberg, 2011: pp. 97–119. https://doi.org/10.1007/978-3-642-17370-7_4.

[44] H. Chen, W. Zhang, X. Wang, H. Wang, Y. Wu, T. Zhong, B. Fei, Effect of alkali treatment on wettability and thermal stability of individual bamboo fibers, J. Wood Sci. 64 (2018) 398–405. https://doi.org/10.1007/s10086-018-1713-0.

[45] G. Cantero, A. Arbelaiz, R. Llano-Ponte, I. Mondragon, Effects of fibre treatment on wettability and mechanical behaviour of flax/polypropylene composites, Compos. Sci. Technol. 63 (2003) 1247–1254. https://doi.org/10.1016/S0266-3538(03)00094-0.

[46] M.F. Pucci, P.J. Liotier, S. Drapier, Capillary effects on flax fibers - Modification and characterization of the wetting dynamics, Compos. Part A Appl. Sci. Manuf. 77 (2015) 257–265. https://doi.org/10.1016/j.compositesa.2015.03.010.

[47] R. Masoodi, E. Languri, A. Ostadhossein, Dynamics of liquid rise in a vertical capillary tube, J. Colloid Interface Sci. 389 (2013) 268–272. https://doi.org/10.1016/j.jcis.2012.09.004.

[48] C.W. Extrand, Forces, pressures and energies associated with liquid rising in nonuniform capillary tubes, J. Colloid Interface Sci. 450 (2015) 135–140. https://doi.org/10.1016/j.jcis.2015.03.007.

[49] E. Gregersen, The Britannica guide to heat, force, and motion, Britannica Educational Publishing, New York, 2011.

[50] A. Abdelbary, Sliding mechanics of polymers, in: A.B.T.-W. of P. and C. Abdelbary (Ed.), Wear Polym. Compos., Woodhead Publishing, Oxford, 2014: pp. 37–66. https://doi.org/10.1533/9781782421788.37.

[51] A. Moudood, A. Rahman, H.M. Khanlou, W. Hall, A. Öchsner, G. Francucci, Environmental effects on the durability and the mechanical performance of flax fiber/bio-epoxy composites, Compos. Part B Eng. 171 (2019) 284–293. https://doi.org/10.1016/j.compositesb.2019.05.032.

[52] F. Chegdani, M. El Mansori, New Multiscale Approach for Machining Analysis of Natural Fiber Reinforced Bio-Composites, J. Manuf. Sci. Eng. Trans. ASME. 141 (2019) 11004. https://doi.org/10.1115/1.4041326.